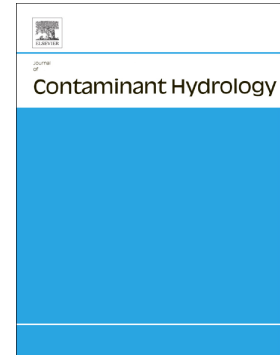


Accepted Manuscript

Effect of material variability and compacted layers on transfer processes in heterogeneous waste rock piles

Belkacem Lahmira, René Lefebvre, Michel Aubertin, Bruno Bussi re



PII: S0169-7722(17)30004-9
DOI: doi: [10.1016/j.jconhyd.2017.07.004](https://doi.org/10.1016/j.jconhyd.2017.07.004)
Reference: CONHYD 3316
To appear in: *Journal of Contaminant Hydrology*
Received date: 12 January 2017
Revised date: 8 June 2017
Accepted date: 15 July 2017

Please cite this article as: Belkacem Lahmira, René Lefebvre, Michel Aubertin, Bruno Bussi re , Effect of material variability and compacted layers on transfer processes in heterogeneous waste rock piles. The address for the corresponding author was captured as affiliation for all authors. Please check if appropriate. Conhyd(2017), doi: [10.1016/j.jconhyd.2017.07.004](https://doi.org/10.1016/j.jconhyd.2017.07.004)

This is a PDF file of an unedited manuscript that has been accepted for publication. As a service to our customers we are providing this early version of the manuscript. The manuscript will undergo copyediting, typesetting, and review of the resulting proof before it is published in its final form. Please note that during the production process errors may be discovered which could affect the content, and all legal disclaimers that apply to the journal pertain.

Journal of Contaminant Hydrology

**Effect of material variability and compacted layers on transfer processes in
heterogeneous waste rock piles**

Belkacem Lahmira^{*1,2}, René Lefebvre², Michel Aubertin³, Bruno Bussière⁴

¹Department of Civil and Environmental Engineering, Carleton University, Ottawa, Ontario, Canada (formerly at INRS-ETE)

²Institut national de la recherche scientifique, Centre Eau Terre Environnement (INRS-ETE), Québec, Québec, Canada

³École polytechnique de Montréal, Département des génies civil, géologique et des mines (CGM), Montréal, Québec, Canada

⁴Université du Québec en Abitibi-Témiscamingue (UQAT), Rouyn-Noranda, Québec, Canada

*Corresponding author: belkacem.lahmira@gmail.com

ABSTRACT

The heterogeneity of waste rock piles is due to the wide and variable grain size distribution of waste rock and construction methods leading to complex internal structures. The general objective of this work was to better understand the effect of such heterogeneity on the coupled transfer processes acting within waste rock piles producing Acid Mine Drainage (AMD). For this purpose, parametric numerical simulations were conducted with the TOUGH AMD numerical simulator, considering 1) three random spatial distributions of the same material properties to assess the resulting behavior, 2) four ranges of material properties with the same spatial distribution to evaluate the effect of the degree of heterogeneity, and 3) the effect of compacted layers due to circulation of heavy equipment during construction. Results show that fine-grained (denser with lower permeability) material present near the boundary of a pile can limit air entry. Coarse materials promote preferential flow of gas and water vapor. Fine-grained materials beneath the pile surface favor the internal condensation of water vapor and thus minimize water loss. The initiation of secondary gas convection cells requires a minimal degree of heterogeneity. The presence of coarse grained material in the pile does not necessarily lead to more convection and higher AMD production. The magnitude of convection rather depends on the amount of fine-grained material and its distribution in the pile. Results also show that low-permeability compacted layers strongly limit convection. Results thus support waste rock pile construction methods integrating fine-grained materials or compacted layers to minimize AMD production.

Keywords: Waste rock; acid mine drainage; multiphase fluid flow; preferential flow; heterogeneity; anisotropy.

Abbreviations: AMD stands for acid mine drainage.

1 INTRODUCTION

Waste rock piles producing Acid Mine Drainage (AMD) have been the subject of many studies leading to a better understanding of these complex systems. Previous studies have mainly targeted transfer processes involved in AMD generation (Guo, 1993; Lefebvre, 1994; Newman et al., 1997; Lefebvre et al., 2001a, 2001b; Linklater et al., 2005; Molson et al., 2005; Fala et al., 2006, 2012; Bussière et al., 2011; Amos et al., 2015). These studies have demonstrated that the processes are coupled and their analysis cannot be done separately. Subsequently, research in this area has focused on developing environmental protection methods (Wilson et al., 2000b; Fala et al., 2005, 2006; Aubertin et al., 2005; Aubertin, 2013; Martin et al., 2005; Molson et al., 2005, 2008; Dawson et al., 2009; Raykaart and Hockley, 2009; Lefebvre et al. 2011; Lahmira et al. 2014a, 2014b; Broda et al., 2015). For new sites, the choice of a waste rock pile construction method is related to practical considerations and economic constraints, in addition to environmental issues (Wels et al., 2003).

The end-dumping and push-dumping construction methods involve the discharge of waste rock materials at the top of slopes (Morin et al., 1991; Fala, 2002; Aubertin et al., 2002a; Aubertin, 2013). These methods promote particles segregation, alternated layers with different particle size and the formation of tilted stratified layers (Wilson et al., 2000a; Aubertin et al., 2002a, 2002b; Anterrieu et al., 2007, 2010; Azam et al., 2007; Smith et al. 2013b, 2013c). When pile construction includes benches, the repeated passage of heavy machinery over each bench surface causes the creation of a compacted layer that persists within the pile during construction (Aubertin et al., 2002a, 2002 b, 2005; Nichol, 2002; Martin et al., 2005; Aubertin, 2013; Dawood and Aubertin, 2014). The internal structure resulting from the construction method thus directly

affects fluid circulation within the pile (Fala et al., 2005, 2012; Dawood and Aubertin, 2009, 2014; Neuner et al., 2013; Amos et al., 2015) and therefore AMD generation.

Using numerical simulations, Lahmira (2010) and Lahmira et al. (2016) have shown the effects of heterogeneity and anisotropy on transfer processes in waste rock piles. These include: i) a random arrangement of materials with different hydraulic properties leads to preferential flow of water and gas within the pile; ii) fluids circulate through separate pathways, with water flowing preferentially through the finest materials (with high water saturation) whereas more gas flows through coarser materials; iii) the anisotropy related to the pile construction method produces different gas flow patterns and oxygen supply rates, with benches favoring horizontal exchanges and air entry through the slope of the pile, whereas end-dumping and push-dumping promote gas entry from the pile surface.

The mineralogical composition of materials can also affect the global behavior of a pile containing reactive minerals (Gerke et al., 1998; Lefebvre et al., 2001a, 2002b; Ritchie, 2003; Sracek et al., 2004; Smith et al., 2013a). The waste rock composition and reactivity related to the AMD production are also heterogeneously distributed in waste rock piles (Molson et al., 2005; Lahmira, 2010; Fala et al., 2012; Amos et al., 2015).

For two distinct internal structures (material anisotropies) related to pile construction methods by benches or end-dumping (or push-dumping), the spatial distribution of material properties is considered from three perspectives in this investigation: i) the effect of different spatial distributions with the same materials; ii) the effect of the degree of heterogeneity arising from

the spread of material property values with different fine fractions (fine grained material); and
iii) the effect of adding compacted layers in the pile. Numerical simulations are used to assess these effects on fluid flow and transfer processes, especially oxygen supply along the outer edge of a pile.

2 APPROACH AND METHODOLOGY

The geology, rock extraction techniques, construction method, and site topography are the main sources of heterogeneity within waste rock piles. Such heterogeneity was observed in several pile characterization and monitoring studies (Morin and Hutt, 1994; Gerke et al., 1998; Nichol et al., 2000; Fala, 2002; Nichol et al., 2005; Stockwell et al., 2006; Anterrieu, 2006; Anterrieu et al., 2007, 2010; Dawood et al., 2011; Lefebvre et al., 2012). Waste rock piles have a coarse nature with widely distributed grain-size, from silt to boulders. Piles can be constructed in different ways, depending on topography, available equipment and the nature and quantity of extracted waste rock (Morin et al., 1991; Wilson et al., 2000b; Aubertin et al., 2002a, 2002b; Dawood and Aubertin, 2009). The mode of deposition is often at the origin of features of the internal structure and the type of anisotropy that affect fluids flow. The deposition method by benches involves the superposition of layers that generates a global horizontal permeability greater than the vertical component of permeability in the pile. This method can promote air (oxygen) entry through the slopes of the pile (Aubertin et al., 2002b, 2005; Martin et al., 2005; Molson et al., 2005; Lahmira et al., 2007, 2016 ; Lahmira, 2010; Lahmira and Lefebvre, 2015). On the contrary, a pile built mainly by end-dumping (or push-dumping) is characterized by an anisotropy producing a vertical flow component greater than the horizontal component (Morin et al., 1991; Wilson et al.,

2000b; Aubertin et al., 2002a; Anterrieu, 2006; Anterrieu et al., 2007; Lahmira, 2010; Lahmira et al., 2016).

Lahmira et al. (2007) and Lahmira et al. (2016) have shown that heterogeneity and anisotropy induced by the construction method have a major impact on transfer processes in waste rock piles. However, their results were limited to a single spatial distribution of materials with a fixed range of properties for pile construction by benches and end-dumping. It is therefore necessary to evaluate the additional influence of the variability of material properties on transfer processes within heterogeneous piles. For that purposes, such variability is considered from two perspectives:

- A pile built with the same materials but having different spatial distributions, which may lead to significantly different behaviors. The spatial distribution of materials in a pile results from the random placement of materials during construction. The spatial distribution of materials in piles thus defy stratigraphy principles applicable to natural sediments (superposition and continuity), since it results from a random process. To represent this effect, random selections were used to assign different properties to four types of materials in the numerical model cells;
- The effect of the degree of heterogeneity due to different ranges of material property values that can result from the presence of different material types containing varying proportions of fine-grained particles. For this purpose, four types of materials, having the same spatial distribution but different ranges of material properties (between the coarsest

and finest), have been considered. This variability in material properties affects the ranges of both permeability and capillary (water retention) properties (related to grain sizes). In this case, different ranges of properties were assigned to four types of material at the same location in the numerical model cells (same spatial distribution).

Based on the [van Genuchten \(1980\)](#) water retention model, [Table 1](#) shows the different distributions of hydraulic properties assigned to the material types for the four cases considered, with different grain sizes (Coarse, Intermediate, Fine and Very Fine). The anisotropy (k_h/k_v) of these materials depends on the construction method (benches or end-dumping). [Table 2](#) lists the equivalent global properties for homogeneous systems. These cases were also simulated for comparison but these results are not presented in this paper (see results in [Lahmira, 2010](#)). Equivalent homogeneous properties were also assigned to the elements located at the surface (atmospheric elements) and at the base (saturated elements) of the numerical grid to facilitate the imposition of boundary conditions. [Table 3](#) summarizes other properties related to pyrite oxidation rate, fluids flow, heat transfer, and gas diffusion. Whatever the spatial distributions (identified as T1, T2, and T3), the values of the properties given in [Table 3](#) are considered the same in all simulated cases (cases A, B, C and D) to facilitate comparison between these cases.

The material properties for the base case (case C) were used to study the effect of varying spatial distributions of materials. Three spatial distributions (T1, T2, and T3) were selected for the numerical simulations ([Fig. 1](#)). Material properties are kept the same, so the differences between simulated cases are only due to their distinct spatial distributions. As stated, this approach facilitates a comparison of results.

To evaluate the effect of the degree of heterogeneity caused by different ranges of material properties, four ranges of properties (cases A, B, C and D, [Table 1](#)) were assigned to the same random distribution of materials T3 (see [Fig. 1](#)). These results will be compared to the "base case" (case C) with the spatial distribution T3. Permeability and water-retention properties have a large influence on the distribution of fluids and transfer processes in waste rock piles ([Pantelis and Ritchie, 1991](#)). These properties were varied to represent the possible range of a waste rock pile ([Table 1](#)). Even though the range goes from coarse to fine, the properties do not necessarily cover the full range that could be found in waste rock piles. The properties used here are representative of systems with globally high permeability in which thermal gas convection is important. The different ranges of properties used in the parametric simulations were selected to assess the following effects:

- **Zones with low permeability:** The presence of low permeability materials is inferred to have a significant effect on transfer processes. Case B includes very fine material (with lower k) compared to cases A, D and C;
- **Degree of heterogeneity:** A greater range of permeability for the four types of material leads to a greater degree of heterogeneity. Case A has the largest range of permeability between the coarser and finer material ratio ($k_{(\text{coarse})} / k_{(\text{fine})} = 50$), making it the most heterogeneous case. Case B is also quite heterogeneous (ratio of 20), while cases C and D are less heterogeneous (ratios of 10).

Case A includes the most permeable material (with case C), while it is also the most heterogeneous model. Materials in case B are less permeable, in terms both of its material and global equivalent permeability ([Table 2](#)). Case C has the most permeable materials, which also

give it the largest equivalent permeability. Case D is intermediate between the other cases. In all cases, anisotropy is the same with a factor of 2 between horizontal and vertical permeability, which depends on construction by benches or end-dumping.

A water infiltration of 350 mm/year (Lefebvre, 1994; Lefebvre et al., 2001b) is imposed at the pile surface for all simulated cases. This recharge is considered as constant and uniform. A change in the recharge between simulations would greatly affect water flow within the pile and the related transfer processes, which would cause ambiguities in the interpretation of results. Furthermore, with a varying recharge, it would be very difficult to identify the effect of permeability and spatial distribution of materials on the transfer processes involved in the generation of AMD. The infiltration of 350 mm/year represents a relative wet climate; thus simulation results may not be representative of different climatic conditions.

The degree of saturation imposed to obtain an infiltration rate of 350 mm/y varied from one case to another, depending on the materials properties and anisotropy (Table 2). A constant temperature (5 °C) and a constant mass fraction of oxygen in air (0.2315) are imposed as boundary conditions along the exterior surface of the pile (Fig. 2). The atmospheric pressure at the top surface is set at 100 kPa and a hydrostatic equilibrium pressure profile is imposed along the slope (immobile air column). These boundary conditions are the initial conditions at the beginning of each simulation. The mass fraction of pyrite is 0.07 and the related density of solid grains is 2740 kg/m³. The volumetric oxidation rate constant K_{ox} is $7.5 \times 10^{-7} \text{ s}^{-1}$ (Lefebvre, 1994; Lefebvre et al., 2001b).

Table 4 gives the effective hydraulic conductivity calculated at mean water saturation for cases A, B, C (base case) and D, according to the spatial distribution of materials (T3) (Lahmira, 2010; Lahmira et al., 2016). These values control the relative infiltration capacity of water in different materials. In **Table 4**, S_{wm} is the mean degree of (water) saturation of the material i ($i =$ Coarse, Intermediate, Fine, Very Fine) under steady-state conditions. The S_{wm} values are obtained as follows:

$$S_{wm} = \frac{\sum S_w^i}{\chi_N^i} \quad [1]$$

where S_w^i is the water saturation for material i under hydrostatic conditions, χ_N^i is the number of appearances of material i in the sample N which is the number of grid elements ($N = 2020$ in this study). For each material i , the hydraulic conductivity is obtained from the following relationship:

$$K_e^i = k^i \cdot k_r^i \cdot \rho \cdot g / \mu \quad [2]$$

where K_e^i is the effective hydraulic conductivity (m/s) of material i ; k^i is the absolute permeability (m^2); k_r^i is the relative permeability (0 to 1); ρ is the water density (1000 kg/m^3); g is the gravitational acceleration (9.81 m/s^2); μ is the dynamic viscosity of water (Pa-s). The relative permeability curve (relative permeability as a function of the degree of saturation) for each material i allows the estimation of the relative permeability (k_r^i) for each material i at the mean water saturation (S_{wm}).

3 NUMERICAL SIMULATION RESULTS

3.1 Varying the random spatial distribution

Figures 3, 4, and 5 show the main conditions obtained after 10 years of simulation for spatial distributions T1, T2 and T3 (base case, i.e. case C) of the four material types considered (Fig. 1) and for the anisotropy related to construction methods by benches and end-dumping. These figures illustrate the most important physical conditions and transfer processes in waste rock piles: a) water saturation and liquid flux; b) temperature and gas flow paths; and c) oxygen mass fraction and total oxygen mass flux. Attention should be paid to the differences in physical conditions and transfer processes that result from the effect of varying the random materials distribution in the pile. The conditions and transfer processes are analyzed for the spatial distribution T3 (base case, Fig. 5) compared with those obtained for spatial distributions T1 (Fig. 3) and T2 (Fig. 4).

The spatial distribution of water saturation and the liquid water infiltration rate vary between cases T1, T2 and T3 (Figs. 3a, 4a, and 5a). This variation is caused by differences in the location of fine-grained materials that largely control water flow. Spatial distribution T2 (Fig. 4) is characterized by more fine elements near the border of the pile than T1 (Fig. 3) and T3 (Fig. 5). This generally induces higher saturations and a significant increase in water flow (Fig. 4a) near the edge of the pile. Such higher water saturation along the outer slope of the pile leads to lower effective air permeability, which reduces air entry and oxygen supply in the pile, thus leading to lower global reaction rates and lower temperatures (as illustrated later).

Temperature distribution (Figs. 3b, 4b, and 5b) for the two spatial distributions T1 and T2 with more fine and very fine grained materials near the outer slope of the pile shows lower maximum temperatures for the construction methods by benches (60 °C, 58 °C) and end-dumping (54 °C, 59 °C) (Figs. 3b and 4b) compared with distribution T3 (base case) (65 °C and 59 °C) (Fig. 5b). This is due to the smaller oxygen supply for cases T1 and T2 induced by higher water saturations near the outer slope of the pile (as stated previously).

The vertical locations of the hottest temperatures for T1 and T2 are also slightly lower than T3 because of the heat carried by water vapor at higher temperatures, which also leads to larger overall gas fluxes. For T3, the downward advective transport of heat related to water infiltration is countered by a strong upward advection of heat in the water vapor. The relative importance of these opposite-acting advective heat transfer processes determines the elevation of the maximum temperature in the pile.

Significant differences are also apparent between T1, T2 and T3 for the distribution of oxygen concentrations and oxygen mass fluxes (Figs. 3c, 4c, and 5c). This is a consequence of the higher effective air permeability near the edge of the pile for T3 due to the absence of finer material that has higher water saturations. This facilitates air flow and thus oxygen supply in the pile, which induces higher temperatures and more pronounced thermal gas convection and atmospheric oxygen intake into the pile (Lahmira, 2010; Lahmira et al., 2016). AMD generation depends on pyrite oxidation that has a first order rate relative to oxygen concentration (Lefebvre et al., 2001a). Thus the base case (T3) (Fig. 5c), which has higher oxygen concentrations compared to

T1 and T2 (Figs. 3c and 4c) would tend to produce more AMD. These results illustrate the coupling between water flow, heat transfer, air flow and AMD generation (oxygen concentration) in a waste rock pile.

In summary, the simulations with different random distributions show that the behavior of a pile can be significantly affected by the materials spatial distribution, particularly along the outer slope. Spatial distributions T1 and T2 show larger water fluxes but lower air convection compared with T3 (base case) due to the presence of finer materials (with a higher degree of saturation) near the edge of the pile. Distributions T1 and T2 (Figs. 3b and 4b) also show lower temperatures and oxygen concentrations compared to the T3 (Fig. 5b) due to limited airflow in the former (Figs. 3c and 4c compared with Fig. 5c). Since oxygen is consumed by pyrite oxidation during its transport in the gas phase within the pile, the smaller inflow of oxygen for cases T1 and T2 leads to less advanced oxygen fronts in the pile compared to case T3 (Fig. 5c).

3.2 Effect of the range of material properties

Different ranges of properties for the four types of material have been considered to evaluate their effect on transfer processes in waste rock piles. The four simulated cases intend to assess the influence of the minimum saturated permeability of materials and the degree of heterogeneity arising from the overall range of materials properties. Results for the base case (case C) are shown in Fig. 5. In the following subsections, an interpretation is made of the simulation results obtained for cases A, B and D. As a reminder, case A includes more permeable materials with a

large range of properties, case B has less permeable materials, and case D considers intermediate properties between those other cases (Tables 1 and 2).

3.2.1 Transfer processes within the pile

Figure 6 illustrates results obtained after 10 years of simulation for case D. Since the range of material permeability for case D is larger than case C (base case), the system retains more water to keep the same effective water permeability in order to sustain the imposed water infiltration rate. This leads to a general increase in water saturation compared with the base case, which is however difficult to detect because of the materials heterogeneity (Fig. 6a compared with Fig. 5a). For case D, the maximum temperatures obtained after 10 years of AMD simulation are about 51 °C and 42 °C for pile construction by benches and end-dumping, respectively (Fig. 6b). These values are relatively low compared to those obtained for case C where the maximum temperatures are 65 °C and 59 °C (Fig. 5b). The oxygen fluxes and its concentrations in case D (Fig. 6c) are also lower than those for case C (Fig. 5c).

Simulation results for case D show that a general reduction in the materials permeability with a relatively modest factor (0.7) is sufficient to change the transfer processes and reduce the ability of gases to circulate in the pile. The air entry is then lower along the slope of the pile, hence reducing the oxygen supply, global oxidation rate, temperature and thermal convection of gases. The hottest zone is also located lower in case D (Fig. 6b) than for case C (Fig. 5b), because of the opposing effects of liquid water and vapor advective heat transfer (as discussed previously).

There are almost no secondary convection cells in case D (contrary to case C) even for the end-dumping model, this leads to little oxygen entering from the pile surface. This indicates that the formation of secondary gas convective cells is closely related to materials permeability and its variation, in addition to anisotropy. The formation of secondary cells appears to require preferential gas flow paths in high permeable materials and sufficient oxygen to increase the local temperature inside the pile and promote thermal gas convection (Figs. 5b and 5c). Other cases leading to the formation of secondary gas convection cells are also assessed below.

The coarse material in case A is as permeable as in case C, but the permeability of the other materials is lower, so case A is the most heterogeneous of the simulated cases (Table 1). The equivalent (homogeneous) permeability for case A is somewhat higher than that of case D (Table 2). Figure 7 shows conditions obtained after 10 years of simulation for case A. Even if the equivalent homogeneous permeability of case A is greater (than for case D), the fine and very fine materials are much less permeable (Table 1) so that water saturation is higher along the preferential pathways of fine and very fine materials (Fig. 7a compared to Fig. 6a).

Referring to the range in permeability values between the coarse and very fine materials (Table 1), water flow is more important in case A (Fig. 7a) because it is more restricted to the fine and very fine materials than in cases D (Fig. 6a) and C (Fig. 5a). These preferential pathways of liquid water flow developed in the fine and very fine materials (where the saturation is very high) are barriers to gas flow in the pile. This situation reduces the airflow and oxygen supply, hence

limiting oxidation, heat production and consequently thermal gas convection (Lahmira and Lefebvre, 2015).

Simulation results for case A show maximum temperatures of about 31 °C and 28 °C for construction by benches and end-dumping, respectively (Fig. 7b). These temperatures are much lower than those obtained for case C (base case, Fig. 5b), there is also a net reduction compared to case D (Fig. 6b). Despite the presence of coarse materials, there is no secondary gas convection cell near the surface of the pile in case A (Fig. 7b). The hottest area (case A) is situated near the base at the edge of the pile, which reflects a dominant advective heat transfer by liquid water infiltration relative to upward advective heat transfer due to water vapor. Oxygen supply is limited to the edge of the pile and does not penetrate deeply (Fig. 7c); which reduces the progress of the oxidation front into the pile.

Case B includes materials with the lowest permeability; the equivalent permeability is also the lowest (Tables 1 and 2). Simulation results illustrate the important role of low permeability and high water retention materials on water saturation, which is higher than for the other simulated cases (compare Fig. 8a with Figs. 7a, 6a, and 5a). Even more than for cases D and A, in case B there is little pore space available for gas flow in case B; this flow is limited by the presence of preferential flow paths with high water saturations. The reduced gas flow in case B limits oxygen supply, such that temperature only increases slightly. After 10 years of simulation, the temperatures are much lower compared to previous cases; the maximum temperature obtained is about 14 °C (Fig. 8b). This cooler temperature reflects a very slow global oxidation rate, which does not produce enough heat to trigger a significant gas convection mechanism. The patterns of

gas flow are simple, from the border slope to the surface of the pile, without distinct principal or secondary gas convection cells (Fig. 8b). The little heat produced is dissipated almost entirely by conduction and also by advection along preferential flow paths (water). The very low convection makes diffusion the most significant oxygen supply mechanism for case B, whereas for other cases convection was the dominant mechanism.

3.2.2 Evolution of average conditions through time

Average simulated conditions in the pile through time provide an overview on the specific behavior and evolution of the pile for the different simulation scenarios. After each time step t and for each element i , TOUGH AMD calculates the conditions representing the system state in terms of temperature, oxygen mass fraction, oxidation rate and remaining pyrite mass fraction. After a given time t , the average conditions are obtained from the following equation:

$$YM_t = \frac{\sum_N Y_t^i \cdot V^i}{\sum_N V^i} \quad [3]$$

N is the number of grid elements, YM_t is the average value of the condition Y calculated after a time t in each grid element (i), V^i is the element volume of the mesh.

Figure 9 shows the evolution of average conditions over time for simulation cases A, B, C and D. The focus is placed on the conditions that give indications on the rate of AMD production, such as temperature, remaining pyrite mass fraction, oxygen concentration, and volumetric oxidation rate. Figure 9 shows that the base case (case C) reached the highest values in terms of average

temperature, oxidation rate, and oxygen mass fraction. The particularity of case C is also irregular in terms of oxygen concentrations and oxidation rate. These variations are caused by the changing locations of secondary convection cells, especially in relation with changes over time in the position of the zone with maximum temperatures towards the inside of the pile. Such secondary cells develop mainly for the case representing the end-dumping construction method, which considers a higher vertical than horizontal permeability. There are fewer irregularities in the curves for the other simulated cases (Fig. 9).

Figure 9 shows that the evolution of average conditions over time is consistent with conditions obtained after 10 years of simulation. Therefore, case D which has a distribution of material properties similar to case C (base case) but with slightly lower permeabilities, shows average characteristics significantly lower than those obtained for case C. Case A, which includes materials with a homogeneous equivalent permeability higher than for case D, but with fine and very fine materials that are less permeable, makes this model very heterogeneous thus limiting gas flow, resulting in lower average temperature, oxygen concentration and oxidation rate. Case B includes too low permeability materials to allow significant gas flow; oxygen supply is mostly by diffusion and temperatures and oxygen concentrations remain low. For case C (base case), the end-dumping model generates higher temperatures and oxygen concentrations compared to the model for construction by benches, indicating that oxygen supply is more pronounced. This is attributed to the formation of secondary convection cells for the case C model with end-dumping. For cases D and A, the construction method by benches leads to higher temperatures, oxygen concentrations and oxidation rate (compared with end-dumping). There is no difference

between the responses for the two construction methods for case B where oxygen supply is dominated by diffusion.

3.3 Effect of compacted layers

Lahmira (2010) conducted simulations made with one, two and three compacted layers; results for three compacted layers are presented here. The effect of these compacted layers applies only for the construction method by benches. Figure 10 illustrates simulation results obtained after 10 years. Preferential flow of water (Fig. 10a) is more significant compared with the base case C (Fig. 5a). Compacted layers show higher water saturations because of their relatively high water retention capacity (i.e. larger air entry value). The maximum temperature reached is 50 °C (Fig. 10b) compared to 65 °C for the base case (Fig. 5b). There is still some thermal convection but it is associated with several convection cells, which depends on the number of compacted layers in the pile (Lahmira, 2010). Figure 10c shows low oxygen concentrations and oxygen fluxes compared to the base case (Fig. 5c). The oxygen concentration tends to decrease with a larger number of compacted layers, and this affects the global oxidation rate. The compacted layers usually remain at high water saturation even during drought periods due to the capillary barrier effect (e.g. Fala et al., 2005). These compacted layers divide the pile into several convection cells instead of a single one. This construction method may reduce the amount of oxidized pyrite and decrease oxygen supply, but it does not stop AMD production (Molson et al., 2005).

4 CONCLUSIONS

The processes involved in the generation of acid mine drainage (AMD) in waste rock piles are complex and interdependent. Numerical modeling was used to assess the effects of heterogeneity

and global anisotropy on these processes, by evaluating specifically the influence of varying spatial distributions of materials and different ranges of material properties. The simulation results presented here are representative of relatively permeable waste rock piles producing AMD, in which thermal convection is important. The water infiltration rate of 350 mm/year used in our model is representative of temperate climates where rainfall and infiltration are relatively large.

The random distributions of the same materials could influence airflow. Air circulation is favored in the absence of a large proportion of fine or very fine materials near the edge of the pile. Simulation results show that different placement of materials can lead to different conditions in a pile, even with the same proportions and the same hydraulic properties. Simulations were also carried out to determine the effect of the range of properties of four types of materials using the same spatial distribution as the base case (case C - distribution T3). The behavior of the pile is controlled by the strong heterogeneity of materials and especially the presence of fine and very fine materials that remain at high water saturations and constitute barriers to gas flow. Simulation results agree with the threshold of 10^{-10} m^2 proposed by Ritchie (1994) as the permeability value below which convection dominates diffusion as a mechanism of oxygen supply.

Results also show that for a pile where there is significant infiltration of water, the effect of advective transport of heat (water infiltration) plays an important role in limiting the rise in temperature if the thermal gas flow (upward) is limited. If waste rock piles contain naturally, or by addition, a significant proportion of fine material with low permeability and high water retention capacity, they will significantly reduce gas flow and consequently reduce the capacity

to generate AMD. These results support the interest of adding fine materials with great contrasts of capillary properties to limit AMD production (Wilson et al., 2000a, 2002; Lahmira and Lefebvre, 2015).

The formation of compacted layers in the case of a pile construction by benches greatly affects the flow of water. These compacted layers retain more water and increase water saturation in the pile due to their high water retention capacity. In contrast, there is a decrease in the pore space for the air flow and oxygen supply. The compacted layers behave more or less as a capillary barrier. The compacted layers divide the convection cell into several cells according to the number of compacted layers present in the pile. Despite this, these compacted layers do not stop gas convection or AMD generation.

Acknowledgements

A NSERC Discovery Grant held by R. Lefebvre and a FRQNT Team Grant held by M. Aubertin supported the doctoral research of Belkacem Lahmira, which included the work reported in this paper.

References

- Amos, R., Blowes, D.W., Bailey, B.L., Segó, D.C., Smith, L., Ritchie, A.I.M., 2015. Waste-rock hydrogeology and geochemistry. *Appl. Geochem.* 57, 140 – 256
- Anterrieu, O., 2006. Caractérisation géophysique de la structure interne d'une halde à stériles (Master Thesis) École Polytechnique de Montréal, Canada.
- Anterrieu, O., Chouteau, M., Aubertin, M., Bussière, B., 2007. A geophysical investigation of the internal structure of a waste rock pile. *Mining and the Environment IV Conference*, October 19-27, Sudbury, Ontario, Canada.

Anterrieu, O., Chouteau, M., Aubertin, M., 2010. Geophysical characterization of the large-scale internal structure of a waste rock pile from a hard rock mine. *Bull. Geol. Eng. Environ.* 69, 533–548.

Aubertin, M., Bussière, B., Bernier, L., 2002a. *Environnement et gestion des rejets miniers*. Les presses internationales de Polytechnique Montreal, Québec (CD-ROM).

Aubertin, M., Fala, O., Bussière, B., Martin, V., Campos, D., Gamache-Rochette, A., Chouteau, M., Chapuis, R.P., 2002b. Analyse des écoulements de l'eau en conditions non saturées dans les haldes à stériles. In *défis et perspectives: Symposium 2002 sur l'Environnement et les Mines* (CD-ROM), Rouyn-Noranda, Canada.

Aubertin, M., Fala, O., Molson, J., Gamache-Rochette, A., Lahmira, B., Martin, V., Lefebvre, R., Bussière, B., Chapuis, R.P., Chouteau, M., Molson, G.W., 2005. Évaluation du comportement hydrogéologique et géochimique des haldes à stériles. *Symposium Rouyn-Noranda: L'environnement et les mines*, mai 2005, Rouyn-Noranda, Proc. On CD-ROM, CIM.

Aubertin, M., 2013. Waste rock disposal to improve the geotechnical and geochemical stability of piles. In: *Proceedings of the World Mining Congress*, Montreal, QC, Canada.

Azam, S., Wilson, G.W., Herasymuik, G., Nichol, C., Barbour, L.S., 2007. Hydrogeological behaviour of an unsaturated waste rock pile: a case study at the Golden Sunlight Mine, Montana, USA. *Bull Eng Environ.* 66, 259-268.

Broda, S., Aubertin, M., Blessent, D., Hirthe, E., and Graf, T., 2015. Improving control of contamination from waste rock piles. *ICE Institution of Civil Engineers – Environmental Geotechnics* <http://dx.doi.org/10.1680/envgeo.14.00023>.

Bussière, B., Demers, I., Dawood, I., Plante, B., Aubertin, M., Peregoedova, A., Penin, G., Lessard, G., Intissar, R., Benzaazoua, M., Molson, J.W., Chouteau, M., Zagury, G.J., Monzon,

- M., Laflamme, D., 2011. Comportement géochimique et hydrogéologique des stériles de la mine Lac Tio. Symposium 2011 sur l'environnement et les mines, Rouyn-Noranda, QC, Canada.
- Dawood, I., Aubertin, M., 2009. A numerical investigation of the influence of internal structure on the unsaturated flow in a large waste rock pile, 62nd Canadian Geotechnical Conference and 10th Joint CGS/IAH-CNC Groundwater Specialty Conference, Halifax, Nova Scotia (2009).
- Dawood, I., Aubertin, M., Intissar, R., Chouteau, M., 2011. A combined hydrogeological–geophysical approach to evaluate unsaturated flow in a large waste rock pile. Proceedings of the 14th Pan-American Conference on Soil Mechanics and Geotechnical Engineering (PCSMGE), 64th Canadian Geotechnical Conference (CGC), and 5th Pan-American Conference on Teaching and Learning of Geotechnical Engineering (PCTLGE), Toronto, ON, Canada, p.8.
- Dawood, I., Aubertin, M., 2014. Effect of dense material layers on unsaturated water flow inside a large waste rock pile: a numerical investigation. *Mine Water Environ.* 33, 24-38.
- Dawson, B., Phillip, M., O’Kane, M., 2009. Sullivan Mine fatalities incident: Site setting, acid rock drainage management, land reclamation and investigation into the fatalities. In: 8th ICARD International Conference on Acid Rock Drainage, Skelleftea, Sweden. 22–26 June 2009. Vol. 3, Swedish Assoc. Mines, Miner., and Metal Prod., Stockholm, p. 1898–1907.
- Fala, O., 2002. Étude des écoulements non saturés dans les haldes à stériles à l’aide de simulations numériques. Master Thesis (M.Sc.A), Génie Minéral, Dép. CGM, École Polytechnique de Montréal, Montréal, QC, Canada.
- Fala, O., Aubertin, M., Molson, J.W., Bussière, B., Wilson, G.W., Chapuis, R., Martin, V., 2003. Numerical modeling of unsaturated flow in uniform and heterogeneous waste rock piles. In: Farrell, T., Taylor, G. (Eds). 6th International Conference on Acid Rock Drainage (ICARD).

Australasian Institute of Mining and Metallurgy, Cairns, Australia, Publications Series 3/2003, pp. 895-902.

Fala, O., Molson, J.W., Aubertin, M., Bussière, B., 2005. Numerical modelling of flow and capillary barrier effects in unsaturated waste rock piles. *Mine Water Environ.* 24(4), 172-185.

Fala, O., Molson, J.W., Aubertin, M., Bussière, B., Chapuis, R.P., 2006. Numerical simulations of long term unsaturated flow and acid mine drainage at waste rock piles. Proceedings of the 7th International Conference on Acid Rock Drainage (ICARD). March 2006, St. Louis, Missouri. The American Society of Mining and Reclamation, pp. 582-597.

Fala, O., Molson, J., Aubertin, M., Dawood, I., Bussière, B., Chapuis R.P., 2012 A numerical modelling approach to assess long-term unsaturated flow and geochemical transport in a waste rock pile. *Int. J. Min, Reclam. and Environ.* <http://dx.doi.org/10.1080/17480930.2011.644473>.

Gerke, H.H., Molson, J.W., Frind, E.O., 1998. Modeling the effect of chemical heterogeneity on acidification and solute leaching in overburden mine spoils, *Journal of Hydrology.* 209, 166-185.

Guo, W., 1993. Numerical simulation of coupled heat transfer and gas flow in porous media with applications to acid mine drainage (Ph.D. thesis), Penn State University, University Park, PA.

Lahmira, B., Lefebvre, R., Aubertin, M., Bussière, B., 2007. Modeling the influence of heterogeneity and anisotropy on physical processes in AMD-producing waste rock piles. Proceedings, OttawaGeo 2007, 60th Canadian Geotechnical Conference and 8th Joint CGS/IAH-CNC Groundwater Conference. Ottawa, ON, Canada. 21-24 Oct. 2007. Can. Geotech. Soc., Calgary, AB.

Lahmira, B., 2010. Numerical Modeling of Physical Processes Affecting the Behaviour of Waste Rock Piles Producing Acid Mine Drainage ([In French]. Ph.D thesis) INRS-Eau, Terre Environnement, Quebec, Canada (476 pp).

Lahmira, B., Barbour, L., Huang, M., 2014a. Numerical modeling of gas flow in the Suncor coke stockpile covers. *Vadose Zone J.* 13 (1). <http://dx.doi.org/10.2136/vzj2013.07.0119>.

Lahmira, B., Lefebvre, R., Hockley, D., Phillip, M., 2014b. Atmospheric Controls on Gas Flow Directions in a Waste Rock Dump. *Vadose Zone J.* 13 (10). <http://dx.doi.org/10.2136/vzj2014.03.0032>.

Lahmira, B., Lefebvre, R., 2015. Numerical modelling of transfer processes in a waste rock pile undergoing the temporal evolution of its heterogeneous material properties. *Int. J. Mining, Reclam. Environ.* 29(6), 499-520. <http://dx.doi.org/10.1080/17480930.2014.889362>.

Lahmira, B., Lefebvre, R., Aubertin, M., Bussière, B., 2016. Effect of heterogeneity and anisotropy related to the construction method on transfer processes in waste rock piles. *Journal of Contaminant Hydrology* 184, 35-49. <http://dx.doi.org/10.1016/j.jconhyd.2015.12.002>.

Lefebvre, R., 1994. Caractérisation et modélisation numérique du drainage minier acide dans les haldes de stériles (Characterization and numerical simulation of acid mine drainage in waste rocks). (In French, Ph.D. Thesis) Université Laval, Quebec City, Canada (June 1994, 375 pp.)

Lefebvre, R., Hockley, D., Smolensky, J., Gélinas, P., 2001a. Multiphase transfer processes in waste rock piles producing acid mine drainage. Part (1): Conceptual model and system characterization. *J. Contam. Hydrol.* 52 (1-14), 137-164 (Special ed. On Practical Applications of Coupled Process Models in Subsurface Environments).

Lefebvre, R., Hockley, D., Smolensky, J., Gélinas, P., 2001b. Multiphase transfer processes in waste rock piles producing acid mine drainage, Part (2): Applications of numerical simulation. *J.*

Contam. Hydrol 52 (1-4), 165-186 (Special ed. On Practical Applications of Coupled Process Models in Subsurface Environments).

Lefebvre, R., Lahmira, B., Löbner, W., 2011. Numerical modeling of gas flow to select a radon emission control method in waste rock dump 38neu, Germany. Proceedings of Geohydro 2011, 1st Joint CANQUA/IAH-CNC Conference, Quebec City, QC, Canada. 28–31 Aug. 2011. Paper 2410.

Lefebvre, R., Lahmira, B., Löbner, W., 2012. Field monitoring and numerical modeling of gas flow and radon emission control in waste rock dump 38neu, Germany. In: Price, W.A., et al. (Eds.), 9th International Conference on Acid Rock Drainage, Ottawa, ON, Canada. 20–26 May 2012. Curran Assoc., Red Hook, NY. pp. 1432–1442.

Linklater, C.M., Sinclair, D.J., Brown, P.L., 2005. Coupled chemistry and transport modeling of sulphidic waste rock dumps at the Aitik mine site, Sweden. *J. Appl. Geochem.* 20, 275–293.

Martin, V., Aubertin, M., Zhan, J., Bussière, B., Chapuis, R.P., 2005. An investigation into the hydrological behavior of exposed and covered waste rock dumps. *SME Trans.* 318 (2005), 139-143.

Molson, J.W., Fala, O., Aubertin, M., Bussière, B., 2005. Numerical simulations of pyrite oxidation and acid mine drainage in unsaturated waste rock piles. *J. Contam Hydrol.* 78 (4), 343-371.

Molson, J.W., Aubertin, M., Bussière, B., Benzaazoua, M., 2008. Geochemical transport modelling of drainage from experimental mine cells covered by capillary barriers. *Applied Geochemistry* 23, 1-24.

- Morin, K.A., Gerencher, E., Jones, C.E., Konasewich, D.E., 1991. Critical literature review of acid drainage from waste rock. MEND Report 1.11.1, Canada Centre for Mineral and Energy Technology.
- Morin, K.A., Hutt, N.M., 1994. An empirical technique for predicting the chemistry of water seeping from mine-rock piles. USBM SP 06 A-94, pp. 12-19.
- Neuner, M., Smith, L., Blowes, D.W., Sego, D.C., Smith, L.J.D., Gupton, M., 2013. The Diavik Waste Rock Project: Water flow through waste rock in a permafrost terrain. *Appl. Geochem.* 36, 222–233. <http://dx.doi.org/10.1016/j.apgeochem.2012.03.011>.
- Newman, L.L., Herasymiuk, G.M., Barbour, S.L., Fredlund, D.G., Smith, T., 1997. The hydrogeology of waste rock dumps and a mechanism for unsaturated preferential flow. 4th International Conference on Acid Rock Drainage (ICARD), pp. 551-564, Vancouver, BC, Canada.
- Nichol, C., Smith, L., Beckie, R., 2000. Hydrogeologic behaviour of unsaturated waste rock: an experimental study. Proceedings of the 5th International Conference on Acid Rock Drainage, Denver, Colorado, USA, pp. 215-224.
- Nichol, C., 2002. Transient flow and transport in unsaturated heterogeneous media: field experiments in mine waste rock (Ph.D. Thesis), University of British Columbia, Canada.
- Nichol, C., Smith, L., Beckie, B., 2005. Field-scale experiments of unsaturated flow and solute transport in a heterogeneous porous medium. *Water Resour. Res.* 41(5), 1-11.
- Pantelis, G., Ritchie, A.I.M., 1991. Macroscopic transport mechanisms as rate-limiting factor in dump leaching of pyritic ores, *Applied Mathematical Modelling* 15 (3), 136-143.
- Raykaart, M; Hockley, D., 2009. Mine waste in clod region, p 119. MEND Report 1.61.5a prepared by SRK Consulting for MEND-Mine Environment Neutral Drainage Program (119 pp).

- Ritchie, A.I.M., 1994. The waste-rock environment. In: Jambor, J.L., Blowes, D.W. (Eds.), Short Course Handbook on Environmental Geochemistry of Sulfide Mine-Wastes, pp 133-161. Mineralogical Association of Canada, Ottawa, Ontario, Canada, pp. 133-161.
- Ritchie, A.I.M., 2003. Oxidation and gas transport in piles of sulphidic material. In: Jambor JL, Blowes, DW, Ritchie, A.I.M (Eds), Environmental Aspects of Mine Wastes, Ch 4, Short Course Vol 31. Mineralogical Association of Canada, pp. 73-94.
- Smith, L.J.D., Bailey, B.L., Blowes, D.W., Jambor, J.L., Smith, L., Segó, D.C., 2013a. The Diavik Waste Rock Project: Initial geochemical response from a low sulfide waste rock pile. *Appl. Geochem.* 36, 210–221. <http://dx.doi.org/10.1016/j.apgeochem.2012.06.008>.
- Smith, L.J.D., Blowes, D.W., Jambor, J.L., Smith, L., Segó, D.C., Neuner, M., 2013b. The Diavik Waste Rock Project: Particle size distribution and sulfur characteristics of low-sulfide waste rock. *Appl. Geochem.* 36, 200–209. <http://dx.doi.org/10.1016/j.apgeochem.2013.05.006>.
- Smith, L.J.D., Moncur, M.C., Neuner, M., Gupton, M., Blowes, D.W., Smith, L., Segó, D.C., 2013c. The Diavik Waste Rock Project: Design and construction of field-scale instrumented waste rock piles. *Appl. Geochem.* 36, 187–199. <http://dx.doi.org/10.1016/j.apgeochem.2011.12.026>.
- Sracek, O., Choquette, M., Gélinas, P., Lefebvre, R., Nicholson, R.V., 2004. Geochemical characterization of acid mine drainage from a waste rock pile, Mine Doyon, Québec, Canada. *Journal of Contaminant Hydrology* 69(1-2), 45-71.
- Stockwell, J., Smith, L., Jambor, J.L., Beckie, R., 2006. The relationship between fluid flow and mineral weathering in heterogeneous unsaturated porous media: A physical and geochemical characterization of a waste-rock pile. *Appl. Geochem.* 21, 1347–1361.

Van Genuchten, M.T., 1980. A closed-form equation for predicting the hydraulic conductivity of unsaturated soils. *Soil Sci. Soc. Am. J.* 44, 892–898.

Wels, C. Lefebvre, R., Robertson, A.M., 2003. An Overview of prediction and control of air flow in acid-generation waste rock dumps. *Proceeding, 6th International Conference on Acid Rock Drainage(ICARD)*, 12-18 July 2003, pp 639-650, Cairns, Australia, Published by The AusIMM, Carlton South, VIC, Australia, pp. 639-650.

Wilson, G.W., Newman, L.L., Ferguson, K.D., 2000a. The co-disposal of waste rock and tailings. *Proceedings of 5th International Conference on Acid Rock Drainage (ICARD)*, Soc. Mining, Metallurgy & Exploration, Inc. (SME), Denver, pp. 789-796.

Wilson, J.A; Wilson, G.W; Fredlund, D.G., 2000b. Numerical modeling of vertical and inclined waste rock layers, *5th International Conference on Acid Rock Drainage*, Soc. Mining, Metallurgy & Exploration, Inc. (SME), Denver.

Wilson, G.W., Wilckland, B., Fines, P., 2002. Concepts for co-mining waste rock and tailings. *Symposium 2002 sur l'environnement et les mines*, 3-5 Novembre 2002, Rouyn-Noranda, QC, Canada.

FIGURE CAPTIONS

Fig. 1. Spatial distributions of materials (T1, T2 and T3) with their water retention curves and unsaturated hydraulic conductivity functions

Fig. 2. Domain discretization and boundary conditions of the numerical model for all simulated cases

Fig. 3. Simulation results after 10 year for the construction by benches (left) and by end-dumping (right), considering the first spatial distribution of materials T1 (see Fig.1)

Fig. 4. Simulation results after 10 year for the construction by benches (left) and by end-dumping (right), considering the second spatial distribution of materials T2 (see Fig. 1)

Fig. 5. Simulation results after 10 year for the construction by benches (left) and by end-dumping (right), considering the third spatial distribution of materials T3 (see Fig. 1) - base case (case C)

Fig. 6. Simulation results after 10 year for case D, construction by benches (left) and by end-dumping (right), considering the third spatial distribution of materials T3 (see Fig. 1)

Fig. 7. Simulation results after 10 year for case A, construction by benches (left) and by end-dumping (right), considering the third spatial distribution of materials T3 (see Fig. 1)

Fig. 8. Simulation results after 10 year for case B, construction by benches (left) and by end-dumping (right), considering the third spatial distribution of materials T3 (see Fig. 1)

Fig. 9. Simulated global averages of physical conditions through time for cases A, B, C and D

Fig. 10. Simulation results after 10 year for the pile with three compacted layers

Table 1. Materials permeability and water retention properties considered in simulation cases (cases A, B, C and D)

Simulation cases	Materials	Construction methods				van Genuchten model parameters	
		Benches		End-dumping		α (kPa ⁻¹)	m (-)
		k_h (m ²)	k_v (m ²)	k_h (m ²)	k_v (m ²)		
Case A	Coarse	5.00x10 ⁻⁰⁹	2.50 x10 ⁻⁰⁹	2.50 x10 ⁻⁰⁹	5.00 x10 ⁻⁰⁹	4.90	0.43
	Intermediate	1.00 x10 ⁻⁰⁹	5.00 x10 ⁻¹⁰	5.00 x10 ⁻¹⁰	1.00 x10 ⁻⁰⁹	2.70	0.30
	Fine	5.00 x10 ⁻¹⁰	2.50 x10 ⁻¹⁰	2.50 x10 ⁻¹⁰	5.00 x10 ⁻¹⁰	1.00	0.32
	Very Fine	1.00 x10 ⁻¹⁰	5.00 x10 ⁻¹¹	5.00 x10 ⁻¹¹	1.00 x10 ⁻¹⁰	0.35	0.30
Case B	Coarse	1.00 x10 ⁻⁰⁹	5.00 x10 ⁻¹⁰	5.00 x10 ⁻¹⁰	1.00 x10 ⁻⁰⁹	4.90	0.43
	Intermediate	5.00 x10 ⁻¹⁰	2.50 x10 ⁻¹⁰	2.50 x10 ⁻¹⁰	5.00 x10 ⁻¹⁰	2.70	0.35
	Fine	1.00 x10 ⁻¹⁰	5.00 x10 ⁻¹¹	5.00 x10 ⁻¹¹	1.00 x10 ⁻¹⁰	1.00	0.32
	Very Fine	5.00 x10 ⁻¹¹	2.50 x10 ⁻¹¹	2.50 x10 ⁻¹¹	5.00 x10 ⁻¹¹	0.35	0.30
Case C (base case)	Coarse	5.00 x10 ⁻⁰⁹	2.50 x10 ⁻⁰⁹	2.50 x10 ⁻⁰⁹	5.00 x10 ⁻⁰⁹	4.90	0.43
	Intermediate	3.50 x10 ⁻⁰⁹	1.75 x10 ⁻⁰⁹	1.75 x10 ⁻⁰⁹	3.50 x10 ⁻⁰⁹	2.70	0.35
	Fine	2.00 x10 ⁻⁰⁹	1.00 x10 ⁻⁰⁹	1.00 x10 ⁻⁰⁹	2.00 x10 ⁻⁰⁹	1.00	0.32
	Very Fine	5.00 x10 ⁻¹⁰	2.50 x10 ⁻¹⁰	2.50 x10 ⁻¹⁰	5.00 x10 ⁻¹⁰	0.35	0.30
Case D	Coarse	3.50 x10 ⁻⁰⁹	1.75 x10 ⁻⁰⁹	1.75 x10 ⁻⁰⁹	3.50 x10 ⁻⁰⁹	4.90	0.43
	Intermediate	2.00 x10 ⁻⁰⁹	1.00 x10 ⁻⁰⁹	1.00 x10 ⁻⁰⁹	2.00 x10 ⁻⁰⁹	2.70	0.35
	Fine	5.00 x10 ⁻¹⁰	2.50 x10 ⁻¹⁰	2.50 x10 ⁻¹⁰	5.00 x10 ⁻¹⁰	1.00	0.32
	Very Fine	3.50 x10 ⁻¹⁰	1.75 x10 ⁻¹⁰	1.75 x10 ⁻¹⁰	3.50 x10 ⁻¹⁰	0.35	0.30

k_h = Horizontal permeability; k_v = Vertical permeability

Table 2. Permeability and water retention properties corresponding to the equivalent global homogeneous systems

Equivalent System	Construction methods				van Genuchten model parameters		Surface water saturation	
	Benches		End-dumping		α (kPa ⁻¹)	m (-)	Benches	End-dumping
	k_h (m ²)	k_v (m ²)	k_h (m ²)	k_v (m ²)				
Case A	1.65×10^{-09}	8.25×10^{-10}	8.25×10^{-10}	1.65×10^{-09}	2.03	0.34	0.290	0.274
Case B	4.13×10^{-10}	2.06×10^{-10}	2.06×10^{-10}	4.13×10^{-10}	2.03	0.34	0.325	0.306
Case C	2.75×10^{-09}	1.38×10^{-09}	1.38×10^{-09}	2.75×10^{-09}	2.24	0.35	0.266	0.253
Case D	1.59×10^{-09}	7.94×10^{-10}	7.94×10^{-10}	1.59×10^{-09}	2.24	0.35	0.278	0.264

k_h = Horizontal permeability; k_v = Vertical permeability

Table 3. Summary of materials properties related to the rate of oxidation, fluid flow, heat transfer and gas diffusion for all materials used in simulation cases A, B, C and D

Simulation cases A, B, C and D						
Properties and Symbols	Units	Materials*				
		C	I	F	VF	HE&S
<u>Properties of the waste rock pile</u>						
Pyrite mass fraction in solid (w_{Py}^{rock})	-	0.07	0.07	0.07	0.07	0.07
Solid density (ρ_s)	kg/m ³	2740	2740	2740	2740	2740
Porosity (n)	-	0.33	0.33	0.33	0.33	0.33
<u>Properties related to the pyrite oxidation rate</u>						
Volumetric oxidation constant (K_{ox})	s ⁻¹	0.75x10 ⁻⁶				
Diffusive/chemical total times (τ_d / τ_c)	-	2.5	2.5	2.5	2.5	2.5
<u>Properties related to the fluid flow</u>						
Water infiltration rate (q_i)	m/y					0.35
Residual water saturation (S_{wr})	-	0.14	0.14	0.14	0.14	0.14
Van Genuchten m factor (m)	-	0.43	0.35	0.32	0.30	0.35
Van Genuchten α factor (α)	kPa ⁻¹	4.9	2.7	1.0	0.35	2.24
<u>Properties related to the heat transfer</u>						
Dry thermal conductivity (λ_d)	W/m °C	0.9	0.9	0.9	0.9	0.9
Sat. thermal conductivity (λ_w)	W/m °C	3.7	3.7	3.7	3.7	3.7
Heat capacity of solid (c_s)	J/kg °C	837	837	837	837	837
Thermal cond. of the base (λ_b)	W/m °C	1.55	1.55	1.55	1.55	1.55
Global density of the base (ρ_b)	kg/m ³	2008.6	2008.6	2008.6	2008.6	2008.6
Heat capacity of the base (c_b)	J/kg °C	1504	1504	1504	1504	1504
<u>Properties related to gas diffusion</u>						
Standard diff. coeff. (D_0)	m ² /s	2.13x10 ⁻⁵				
Temperature diff. coeff. (θ)	-	1.8	1.8	1.8	1.8	1.8
Tortuosity factor (τ)	-	0.7	0.7	0.7	0.7	0.7
Effective oxygen diff. (D_e)	m ² /s	2.85x10 ⁻⁶				

*: C = Coarse; I = Intermediate; F = Fine; VF = Very Fine; HE = Homogeneous Equivalent; S = Surface Material; B = Benches; ED = End-dumping. Abbreviations: Sat. = Saturated; Cond. = Conductivity; diff. coeff. = diffusion coefficient; diff. = diffusivity.

Table 4. Effective hydraulic conductivity K_e (m/s) calculated at mean degree of water saturation (S_{wm}) of different materials according to the materials spatial distribution T3

Materials	Construction methods	Case A		Case B		Case C		Case D	
		S_w	K_e	S_w	K_e	S_w	K_e	S_w	K_e
Coarse	Benches	0.19	1.34×10^{-09}	0.21	1.67×10^{-09}	0.20	2.21×10^{-08}	0.21	5.10×10^{-09}
	End-dumping	0.18	1.46×10^{-09}	0.20	2.04×10^{-09}	0.19	3.87×10^{-09}	0.19	4.50×10^{-09}
Intermediate	Benches	0.32	3.46×10^{-08}	0.34	3.85×10^{-08}	0.28	2.68×10^{-08}	0.29	2.30×10^{-08}
	End-dumping	0.31	4.99×10^{-08}	0.33	4.97×10^{-08}	0.26	2.41×10^{-09}	0.27	1.65×10^{-08}
Fine	Benches	0.46	3.27×10^{-07}	0.49	1.34×10^{-07}	0.35	8.29×10^{-08}	0.38	3.97×10^{-08}
	End-dumping	0.44	4.31×10^{-07}	0.47	1.66×10^{-07}	0.33	7.36×10^{-08}	0.35	3.81×10^{-08}
Very Fine	Benches	0.58	3.72×10^{-07}	0.61	3.06×10^{-07}	0.50	4.66×10^{-07}	0.51	4.22×10^{-07}
	End-dumping	0.55	4.77×10^{-07}	0.58	3.83×10^{-07}	0.47	4.86×10^{-07}	0.49	4.66×10^{-07}

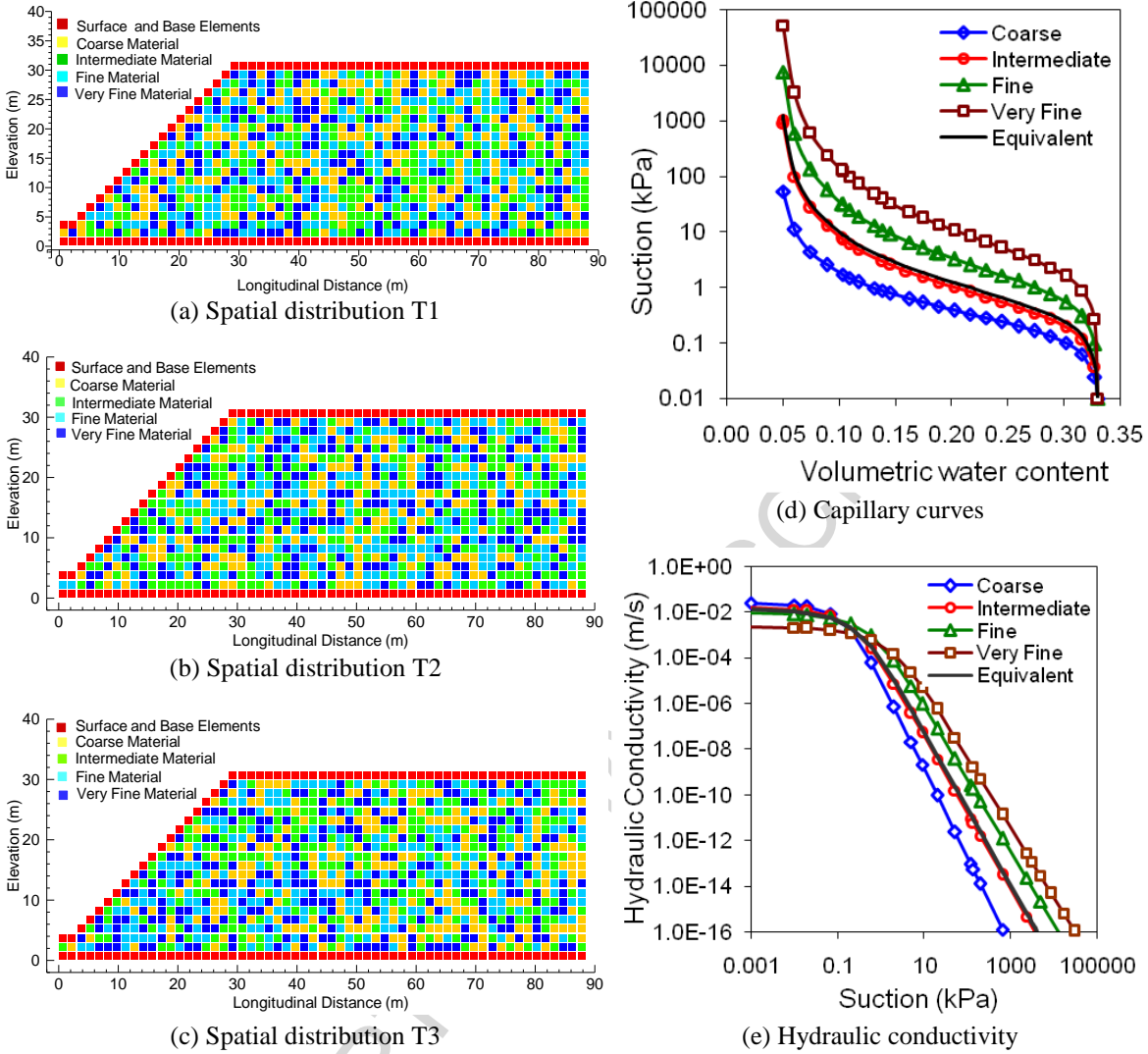


Fig.1. Spatial distributions of materials (T1, T2 and T3) with their water retention curves and unsaturated hydraulic conductivity functions

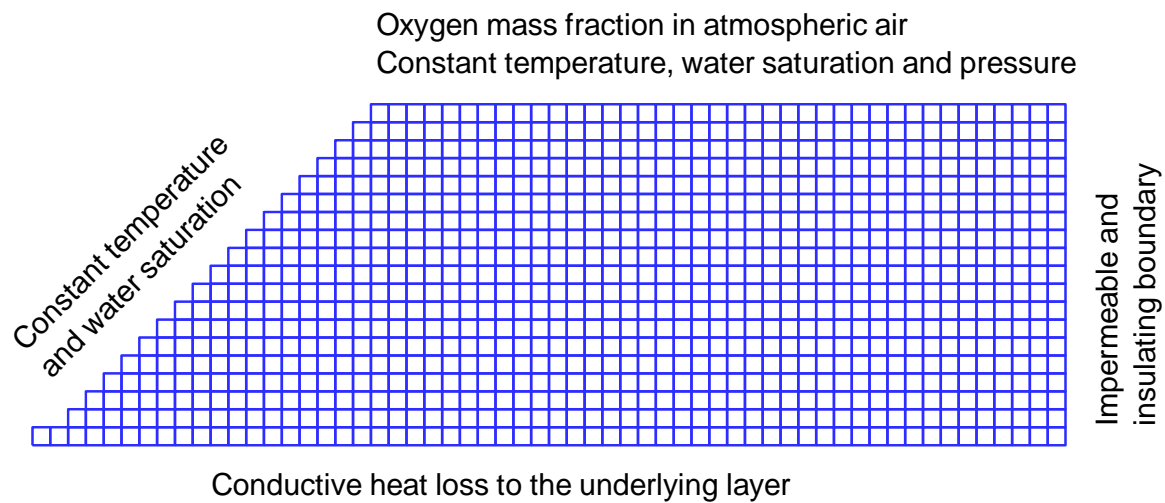


Fig. 2. Domain discretization and boundary conditions of the numerical model for all simulated cases

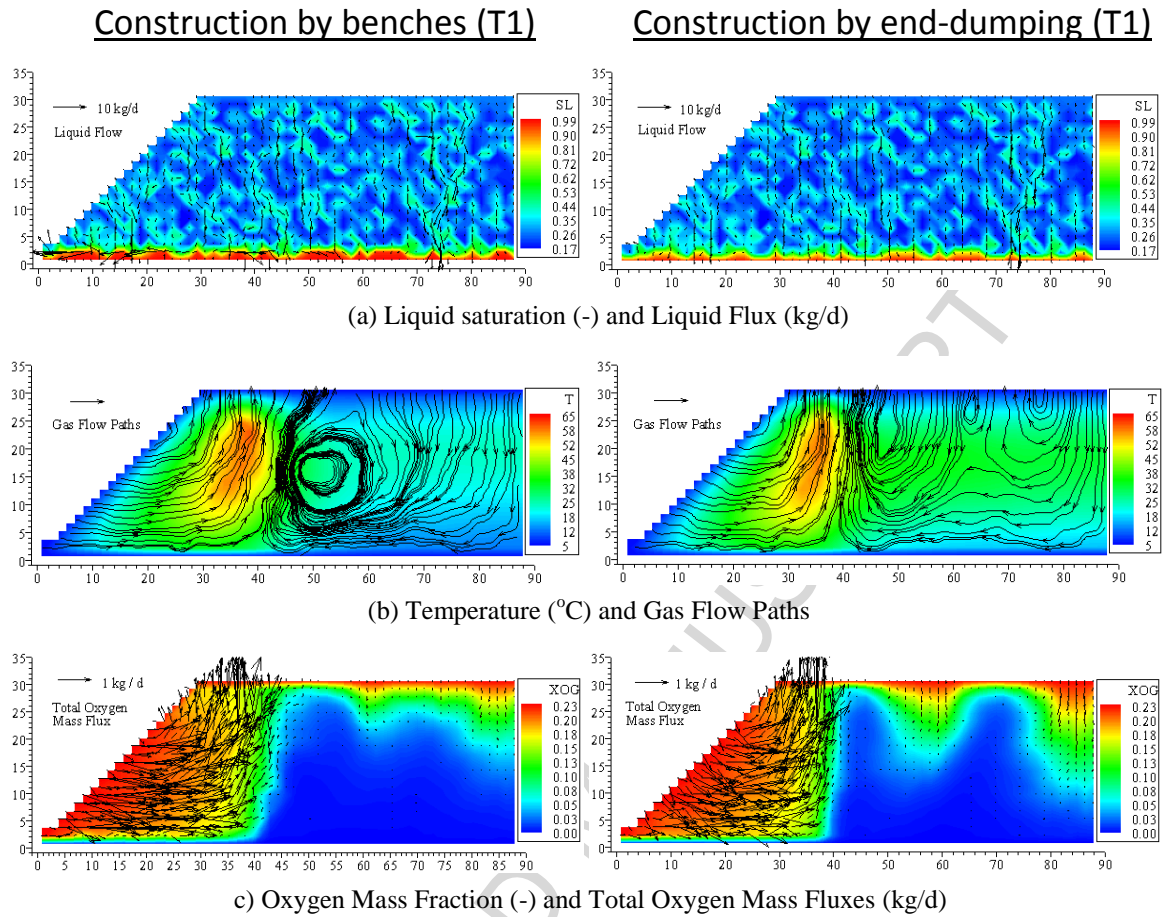
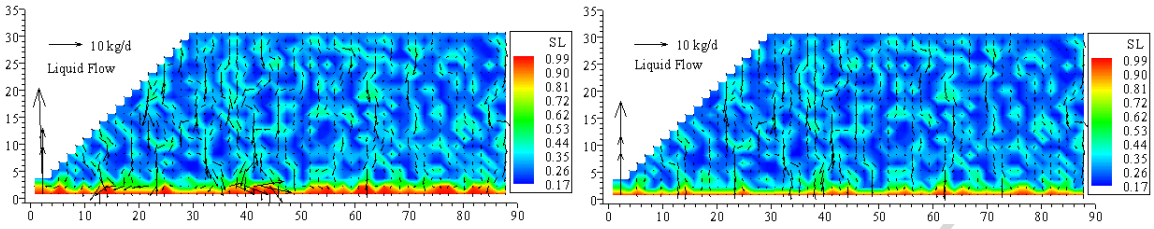


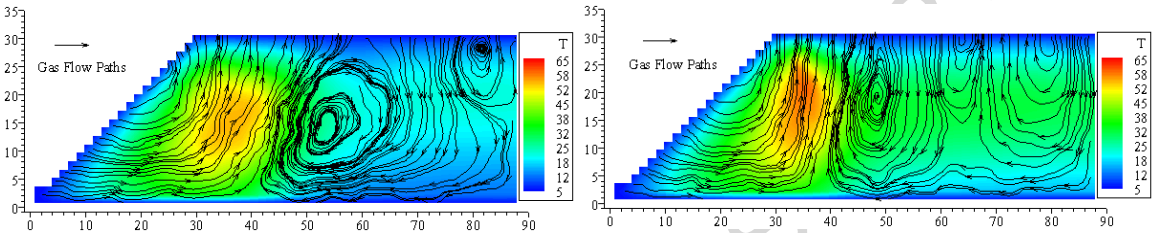
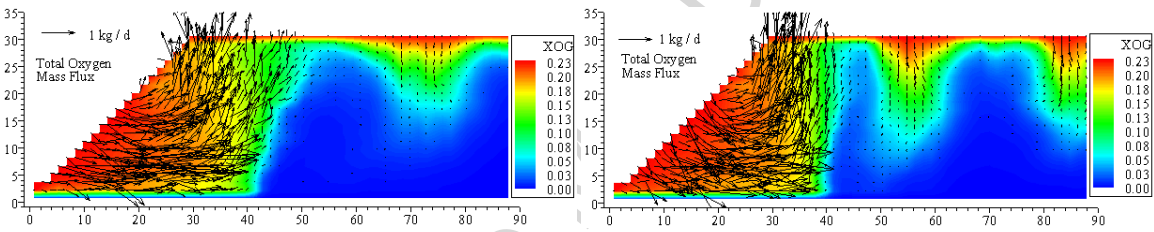
Fig.3. Simulation results after 10 year for the construction by benches (left) and by end-dumping (right), considering the first spatial distribution of materials T1 (see Fig.1)

Construction by benches (T2)

Construction by end-dumping (T2)



(a) Liquid Saturation (-) and Liquid Flux (kg/d)

(b) Temperature ($^{\circ}\text{C}$) and Gas Flow Paths

(c) Oxygen Mass Fraction (-) and Total Oxygen Mass Fluxes (kg/d)

Fig. 4. Simulation results after 10 year for the construction by benches (left) and by end-dumping (right), considering the second spatial distribution of materials T2 (see Fig. 1)

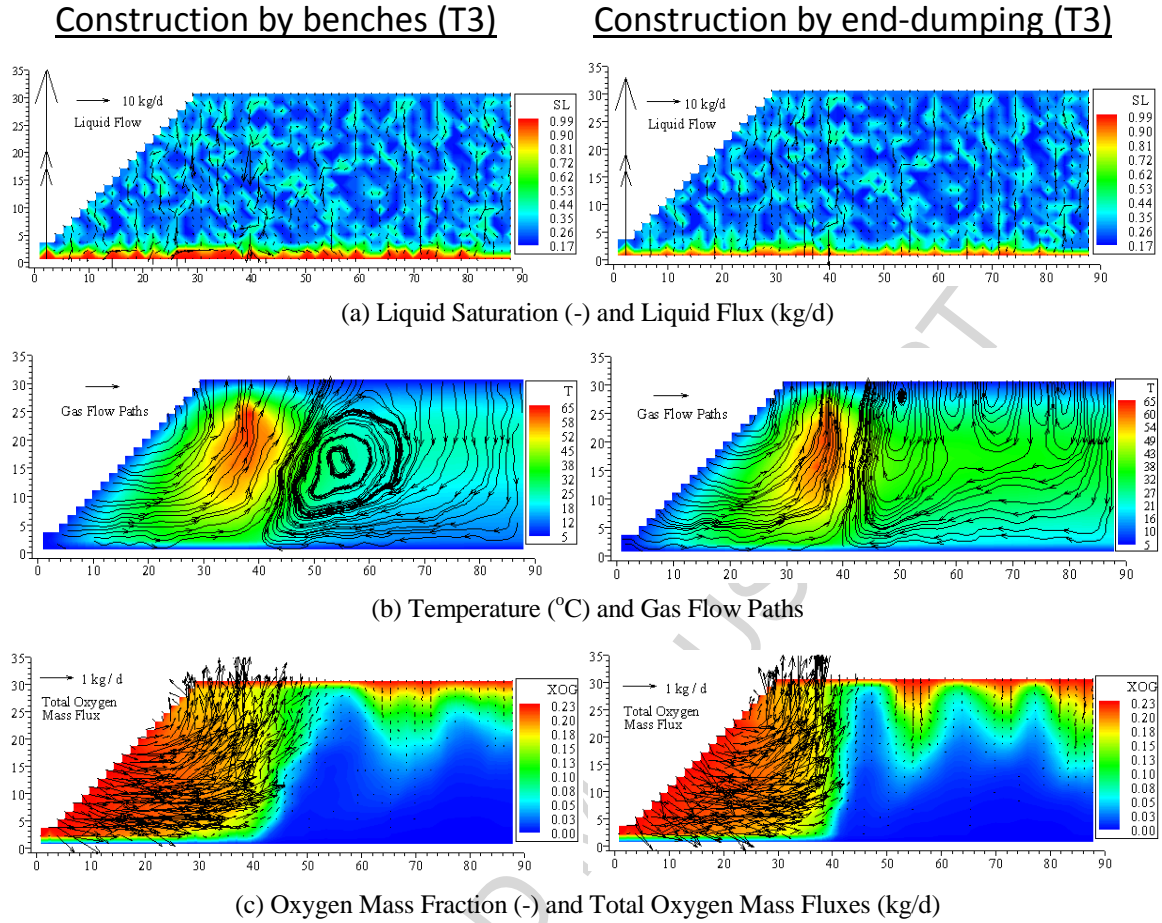
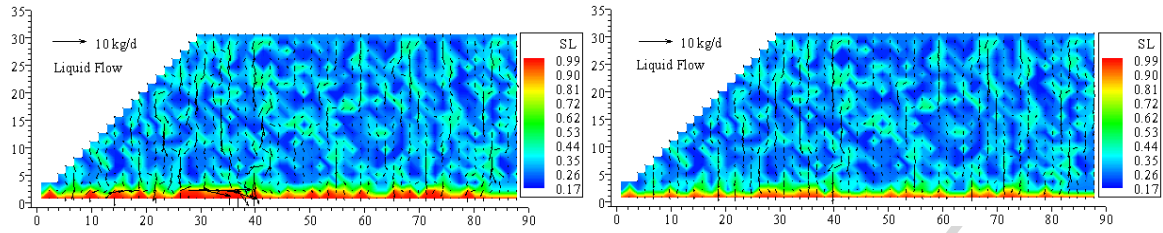
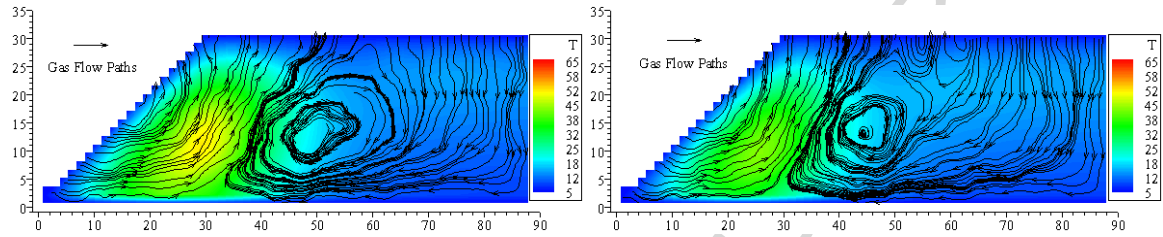


Fig. 5. Simulation results after 10 year for the construction by benches (left) and by end-dumping (right), considering the third spatial distribution of materials T3 (see Fig. 1) - base case (case C)

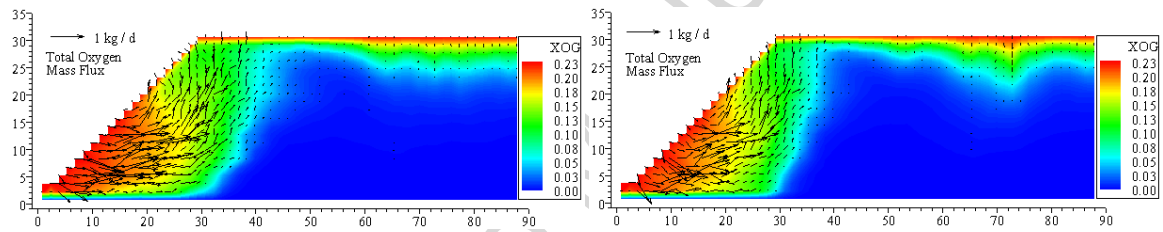
Construction by benches (Case D) **Construction by end-dumping (Case D)**



(a) Liquid Saturation (-) and Liquid Flux (kg/d)



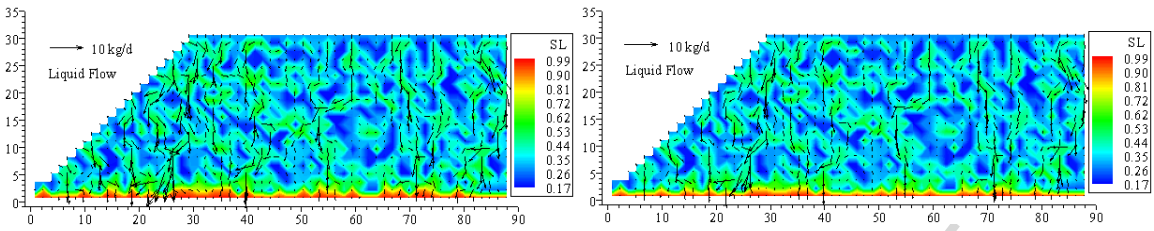
(b) Temperature ($^{\circ}\text{C}$) and Gas Flow Paths



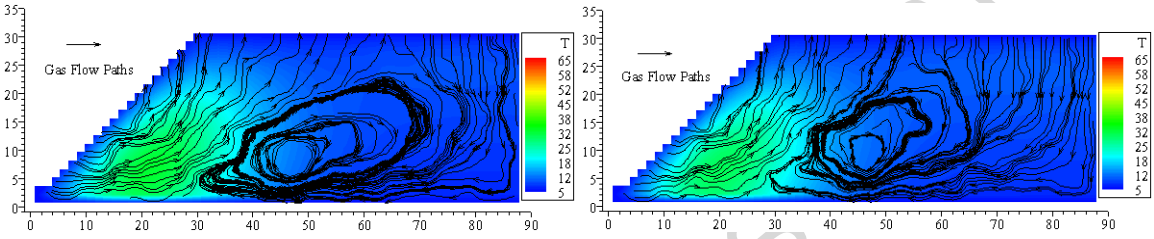
(c) Oxygen Mass Fraction (-) and Total Oxygen Mass Fluxes (kg/d)

Fig.6. Simulation results after 10 year for case D, construction by benches (left) and by end-dumping (right), considering the third spatial distribution of materials T3 (see Fig. 1)

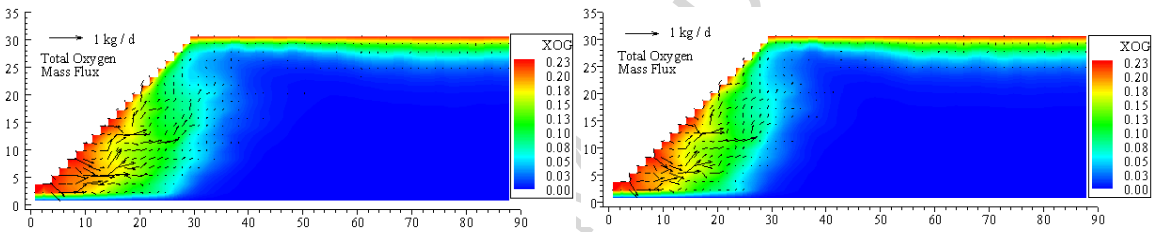
Construction by benches (Case A) Construction by end-dumping (Case A)



(a) Liquid Saturation (-) and Liquid Flux (kg/d)



(b) Temperature ($^{\circ}\text{C}$) and Gas Flow Paths



(c) Oxygen Mass Fraction (-) and Total Oxygen Mass Fluxes (kg/d)

Fig.7. Simulation results after 10 year for case A, construction by benches (left) and by end-dumping (right), considering the third spatial distribution of materials T3 (see Fig. 1)

Construction by benches (Case B) Construction by end-dumping (Case B)

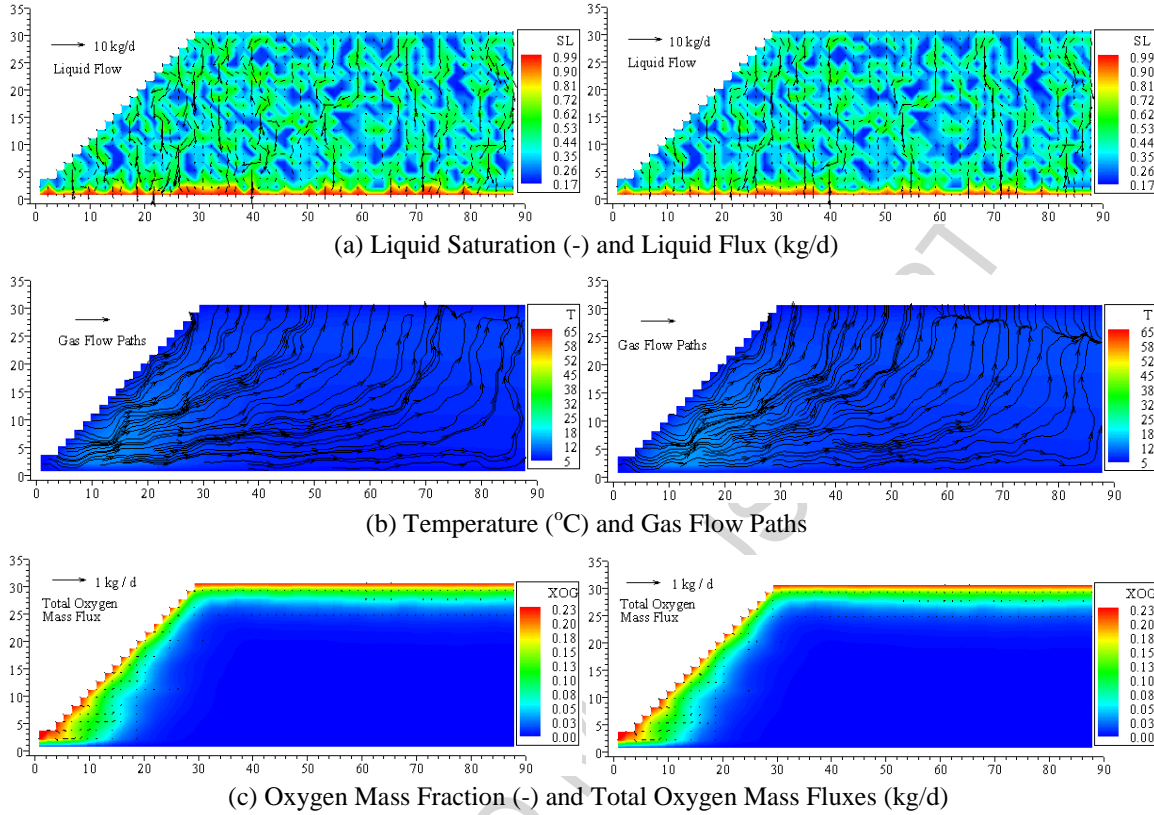


Fig. 8. Simulation results after 10 year for case B, construction by benches (left) and by end-dumping (right), considering the third spatial distribution of materials T3 (see Fig. 1)

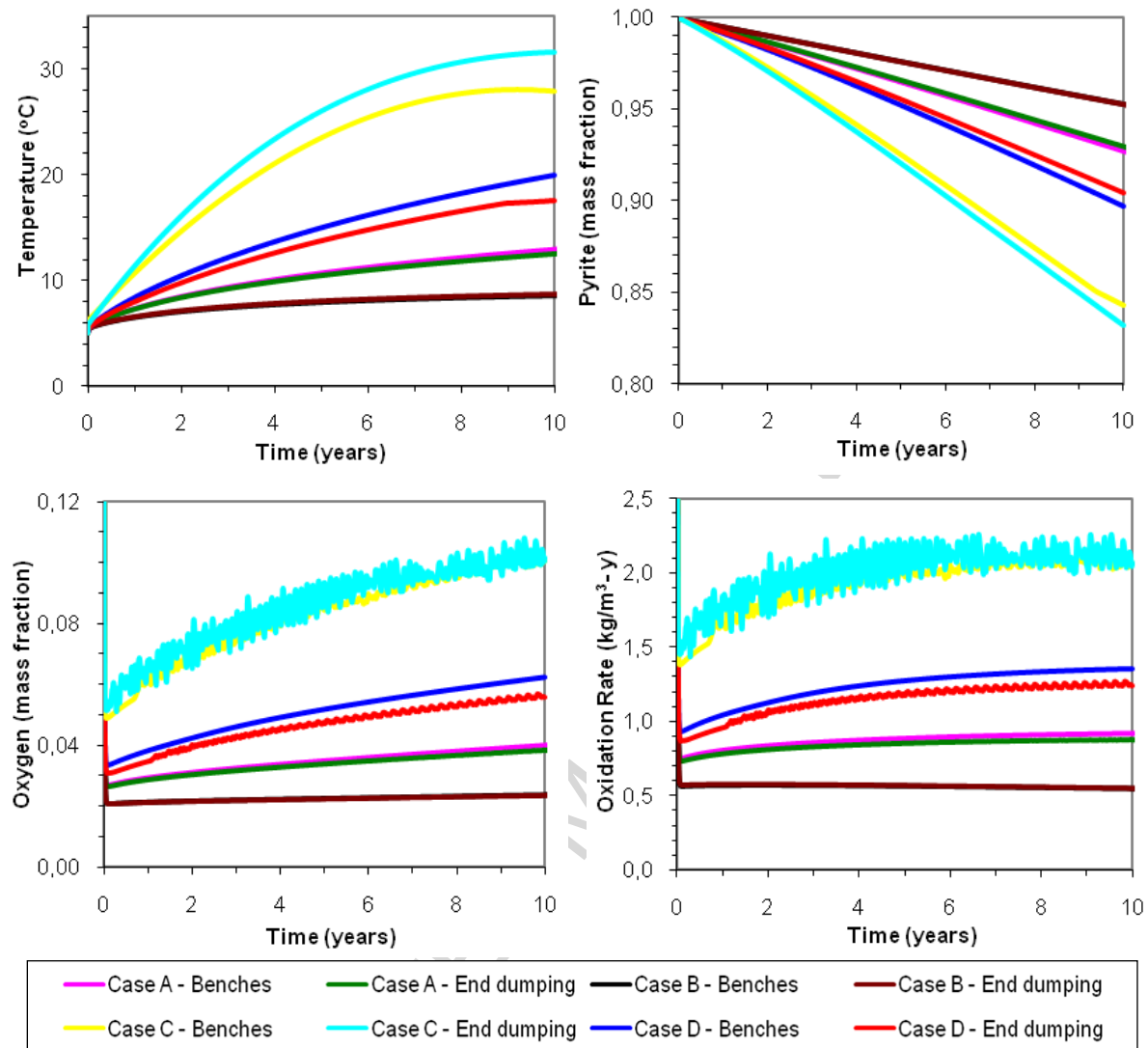


Fig. 9. Simulated global averages of physical conditions through time for cases A, B, C and D

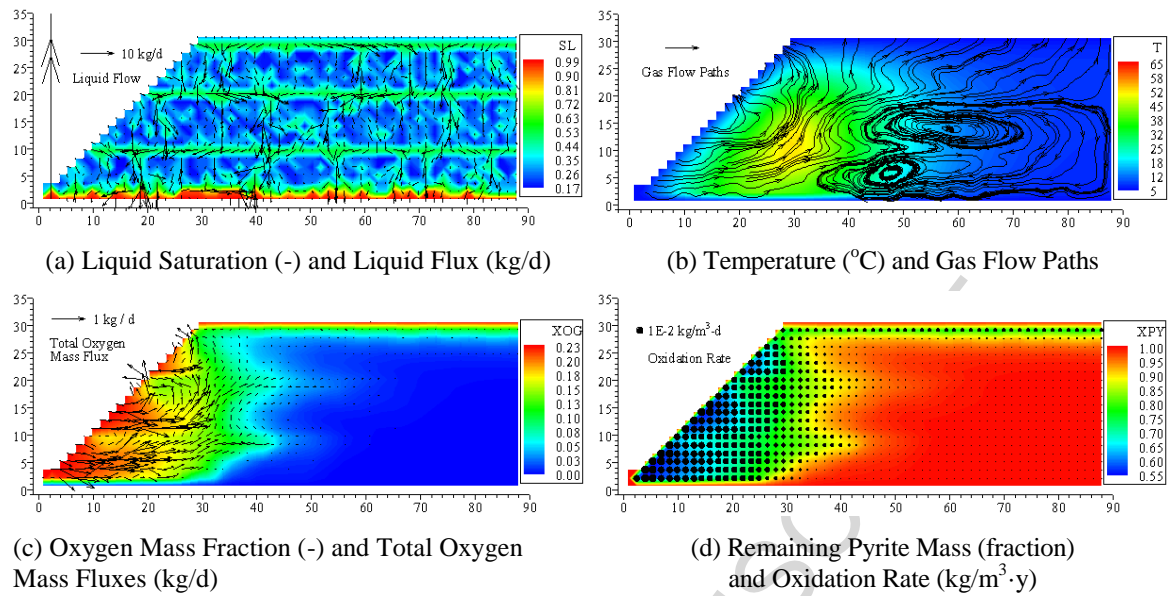


Fig. 10. Simulation results after 10 year for the pile with three compacted layers

Highlights

- Fine-grained material present near the boundary of a pile can limit air entry.
- Fine-grained materials beneath the pile surface favor the internal condensation of water vapor.
- Coarse materials promote preferential flow of gas and water vapor.
- The presence of coarse grained material in the pile does not necessarily lead to more convection and higher AMD production.
- Low-permeability compacted layers strongly limit convection.

ACCEPTED MANUSCRIPT